Velocity-Potential Boundary-Field Integral Formulation for Sound Scattered by Moving Bodies

M. Gennaretti[1], G. Bernardini[2] and C. Poggi[3]
Roma Tre University, Rome, Italy, 00146

C. Testa[4]
CNR-INSEAN, Rome, Italy, 00128

This paper presents a boundary-field integral formulation suitable for the prediction of noise scattered by moving bodies. Although based on the same flow modeling assumptions, linear formulations derived from velocity potential or pressure disturbance wave equations provide different predictions when the scatterer is not at rest. Indeed, the discrepancies reside in the different influence of the neglected nonlinear terms. Here, a velocity potential-based approach is developed by extracting the first-order contributions from the nonlinear terms. This yields a linearized boundary-field, frequency-domain formulation for the scattered potential that, extending the standard linear boundary integral approach, takes into account the effects of mean flow nonuniformity. The influence of the additional field contributions is examined for different scatterer velocities, with the aim of assessing the domain of validity of the fully linear formulation and the rate of growth of the field contributions with increase of velocity. Specifically, the numerical investigation concerns the noise scattered by a moving, non-lifting wing, when impinged by an acoustic disturbance generated by a co-moving point source.

---

[1] Full Professor, Department of Engineering, m.gennaretti@uniroma3.it.
[2] Assistant Professor, Department of Engineering, g.bernardini@uniroma3.it.
[3] PhD Student, Department of Engineering, caterina.poggi@uniroma3.it.
[4] Researcher, Rotary-wing Propulsion and Acoustics Dept., claudio.testa@cnr.it.

Nomenclature

A_i	= Perturbation source intensity
$A_1, A_2, \mathbf{A}_3, \mathbf{A}_4, \mathbf{A}_5$	= Coefficients of the linearized field terms
$\mathbf{C}^{SS}, \mathbf{C}^{VS}, \mathbf{B}^{SS}, \mathbf{B}^{VS}$	= Body-surface influence coefficient matrices
$\mathbf{C}^{SV}, \mathbf{C}^{VV}, \mathbf{B}^{SV}, \mathbf{B}^{VV}$	= Field influence coefficient matrices
c, c_0	= Local and undisturbed-medium speed of sound
c_w	= Wing chord length
k	= Wave number, ω/c_0
G	= Free-space Green's function in body-fixed frame
L	= Wing semi-span length
$\mathbf{M}, M$	= Mach number vector and magnitude
$\mathbf{n}$	= Outward unit normal from body surface
p_i, p_s	= Incident and scattered pressure
$p', \bar{p}'$	= Acoustic pressure and generalized acoustic pressure
p'_i, p'_s	= Incident and scattered acoustic pressure
$\hat{p}$	= Gauge pressure
r_β	= Green's function observer-source distance factor in body-fixed frame
$\hat{r}$	= Observer-source distance covered by potential/pressure signals, $c_0\theta$
$\mathcal{S}$	= Body surface
$\mathbf{v}, \mathbf{v}_p, \mathbf{v}_i, \mathbf{v}_s$	= Total, perturbation, incident and scattered velocity fields
$\mathbf{v}_{st}$	= Reference velocity (nonuniform steady mean inflow in body-fixed frame)
$\mathbf{v}_B$	= Body velocity
$\mathbf{x}, \mathbf{y}$	= Observer and source positions in body-fixed frame
$\mathbf{x}_i$	= Perturbation source position in body-fixed frame
$\mathbf{x}_c$	= Center of wing mid-span cross section
$\mathcal{V}$	= Control volume surrounding the body
γ	= Ratio of specific heat coefficients, c_p/c_v
θ	= Time delay

μ = Linearized field terms

$\boldsymbol{\xi}$ = Position vector in medium-fixed frame

$\boldsymbol{\xi}_x, \boldsymbol{\xi}_y$ = Observer and source positions in medium-fixed frame

$\phi, \phi_p, \phi_i, \phi_s$ = Total, perturbation, incident and scattered velocity potential fields

ϕ_{st} = Reference velocity potential (steady in body-fixed frame)

$\boldsymbol{\phi}_s^S, \boldsymbol{\phi}_s^V$ = Vectors of scattered velocity potential at body surface and field centroids

$\boldsymbol{\phi}_i^S, \boldsymbol{\phi}_i^V$ = Vectors of incident velocity potential at body surface and field centroids

ρ, ρ_0 = Local and undisturbed-medium density

σ = Nonlinear field terms

ω = Angular frequency

I. INTRODUCTION

An obstacle or medium inhomogeneity in the path of a noise wave causes scattering, namely secondary sound spread in a variety of directions. This phenomenon becomes relevant when the wavelength of the impinging acoustic wave is comparable with a characteristic size of the scatterer (solid bodies, interfaces between different media, etc.). As a consequence of the wave-scatterer interaction, the features of the overall pressure field in terms of magnitude, waveform, and directivity may significantly differ from those of the noise field in unbounded space [1].

Sound scattering is a relevant issue in a wide range of engineering applications dealing with stationary and moving objects. For instance, in aeronautics, the analysis of scattering phenomena is of interest both for noise pattern simulation and for the prediction of fuselage wall vibrations that are source of airborne cabin noise. The same phenomena are of interests in ship hydroacoustics for problems concerning sea acoustic pollution and impact on marine life, noise emission regulations, and acoustic detectability of warships.

In principle, the analysis of acoustic scattering is conceived as a problem where the impinging pressure wave is independent of the presence of the scattering surface. This assumption allows to split the noise field into incident and scattered components avoiding, in addition, time-consuming computations where both the source of sound and the scatterer body are considered jointly. Several

configurations of interest comply with it: for instance, propeller-driven aircraft in cruise flight, where the main source of noise (the propeller) is practically aerodynamically independent of the rest of the vehicle; helicopters in flight conditions for which the fuselage is not massively impinged by the main-rotor wake; hull-propeller(s) configurations where strong vortical structures released by the hull do not impact propeller blades. Under these operating conditions, the incident pressure field may be computed by prior aero/hydrodynamic and aero/hydroacoustic analyses of the noise source as if it were isolated, with the rest of the bodies appearing in the evaluation of the scattered acoustic field.

The wide literature concerning sound scattering problems (see, for instance, Refs. [2]-[10]) shows that the scattered pressure field is typically predicted through linear approaches based on boundary integral formulations solving the Helmholtz equations for the velocity potential or the acoustic pressure. Beside them, alternative formulations based on the linear version of the Ffowcs Williams and Hawkings equation have been proposed [11]-[13]. These extend the use of the acoustic analogy to scattering problems either through time-domain approach (the equivalent source method introduced in Ref. [12]), or frequency-domain methodologies [11, 13]

The Helmholtz formulations (for pressure and velocity potential) and the methodologies based on the linear Ffowcs Williams and Hawkings equation provide fully equivalent results, as long as the scattering body is at rest. However, significant discrepancies arise when the body moves: the higher the Mach number, the more significant are the differences among the outcomes given by these linear approaches. This result is highlighted in Ref. [11], where the sound scattered by a wing in uniform translation is predicted both by the frequency-domain approach based on the Ffowcs Williams and Hawkings equation there presented and by a linear velocity potential formulation. Observing that these scattering formulations come from the same potential-flow modelling assumptions, it is deduced that the discrepancies reside in the different influence of the neglected nonlinear terms, the complete pressure and velocity-potential formulations being fully equivalent [14]. However, at present, it is unclear in which of the above mentioned linear scattering formulations the inclusion of the nonlinear terms would give rise to less influential contributions, and the dependency of these terms on body velocity. In this context, enhanced linear approaches are provided by those acoustic

scattering formulations that include nonuniform potential flow effects due to scatterer constant-velocity motion (see, for instance, Refs. [15]-[20]).

In order to assess the impact of nonlinearities on moving-body acoustic scattering predictions (typically provided in the frequency domain), suited formulations extracting their first-order contributions with respect to a steady reference unperturbed configuration should be developed. This process, applicable to the wave equations for the velocity potential (VP), the Lighthill equation (LE) and the Ffowcs Williams and Hawkings equation (FWHE), would give rise to linearized boundary-field, frequency-domain formulations, with proposed new terms from suitably-sized volumes surrounding the scatterer [14]. It is worth reminding that these scattering formulations are fully equivalent only if the nonlinearities are fully retained: however, second-order terms in small perturbation problems (like acoustic scattering) may be suitably considered negligible.

These considerations have drawn the guidelines of the research activity presented here. A novel boundary-field integral formulation for acoustic scattering described in terms of velocity potential is developed and applied. First, the inhomogeneous wave equation for the velocity potential is re-written in terms of superposition of the steady flow field associated to the body motion with the incident and scattered fields. Then, a linearization process is applied and the resulting differential operator for the scattered potential is solved through a boundary-field integral formulation, followed by application of a boundary element method (BEM) (a similar solution process was applied in the past for the aeroelastic stability analysis of wings in transonic flows [21]). As it will be outlined afterwards, the linearized field terms take into account the effects of the nonuniform mean flow due to the steady potential field on sound scattering, extending the widely-applied scattering formulations based on low Mach number and weakly nonuniform flow assumptions [15]-[20].

Goals of the numerical investigation are the assessment both of the influence of the additional field contributions included in the proposed linearized velocity potential formulation, and of the level of accuracy of fully linear VP, LE and FWHE scattering formulations, as compared with the predictions given by the present approach.

In Section II, a proposed new linearized, frequency-domain, boundary-field formulation for the scattered velocity potential is outlined, whereas Section III presents the results of the numerical

investigations concerning the scattering problem already examined in Refs. [11, 22], that consists of a moving, nonlifting wing, impinged by an acoustic disturbance generated by a co-moving source. An outline of the LE and FWHE formulations applied here is provided in Appendix C.

II. THE VELOCITY-POTENTIAL SCATTERING FORMULATION FOR MOVING BODIES

Let us consider a body moving within an inviscid, non-conducting, shock-free flow, that is initially at rest, homentropic and irrotational. Then, the flow remains homentropic and irrotational at all times and the velocity field, $\mathbf{v}$, may be described through the potential, ϕ, such that $\mathbf{v} = \nabla\phi$ [27, 28]. In addition, let us assume that the body is nonlifting, in uniform translation at velocity, $\mathbf{v}_{_B}$, with respect to a frame of reference fixed with the undisturbed medium, while impinged by an incident perturbation velocity potential field generated by external sources. This limits the domain of the scattering problem configurations for which the specific integral formulation presented hereafter is applicable, but does not affect the generality of the proposed approach for the derivation of noise scattering formulations suitable for moving bodies.

Then, combining the continuity equation with the Euler equation, in a frame of reference rigidly connected with the body (body frame, BFR) the velocity potential field is governed by (see Refs. [27, 28] for details)

$$\frac{1}{{c_{_0}}^2}\left(\frac{\partial}{\partial t} - \mathbf{v}_{_B}\cdot\nabla\right)^2\phi - \nabla^2\phi = -\sigma(\phi) + A_i\ \delta(\mathbf{x}-\mathbf{x}_i) \tag{1}$$

where $c_{_0}$ denotes the speed of sound in the undisturbed medium,

$$\sigma(\phi) = \left(1 - \frac{c^2}{{c_{_0}}^2}\right)\nabla^2\phi + \frac{1}{{c_{_0}}^2}\left(\frac{\partial v^2}{\partial t} - \mathbf{v}_{_B}\cdot\nabla v^2\right) + \frac{\mathbf{v}}{2{c_{_0}}^2}\cdot\nabla v^2 \tag{2}$$

collects the nonlinear terms, with $v = \|\mathbf{v}\|$ and c denoting the local speed of sound, and $A_i(t)$ is the intensity of a perturbation source located at the point $\mathbf{x}_i$ placed outside of the region where σ is not negligible.

Note that, although the differential operator is expressed in the BFR, body and flow velocity, $\mathbf{v}_{_B}$ and $\nabla\phi$, are still those observed in a frame of reference fixed with the undisturbed air medium at rest (medium frame, MFR).

A. The boundary-field integral formulation

Following the boundary integral equation method presented, for instance, in Refs. [14] and [27], the velocity potential solution may be formulated through the following boundary-field expression

$$\phi(\mathbf{x},t) = \int_{\mathcal{S}} \left[G\frac{\partial \phi}{\partial \hat{n}} - \phi\frac{\partial G}{\partial \hat{n}} + \frac{\partial \phi}{\partial t}\, G\left(\frac{\partial \theta}{\partial \hat{n}} + 2\frac{\mathbf{M}\cdot\mathbf{n}}{c_0}\right)\right]_\theta \mathrm{d}\mathcal{S}(\mathbf{y}) + \int_{\mathcal{V}} G\,[\sigma(\phi)]_\theta\,\mathrm{d}\mathcal{V}(\mathbf{y}) + \phi_i(\mathbf{x},t) \quad (3)$$

where $\mathcal{S}$ and $\mathcal{V}$ represent, respectively, the scatterer surface and the field domain surrounding the body where the nonlinear terms are not negligible. In this equation

$$G(\mathbf{x},\mathbf{y}) = \frac{-1}{4\,\pi\, r_\beta}$$

is the free-space Green's function of Eq. (1), where

$$r_\beta = \sqrt{[\mathbf{M}\cdot(\mathbf{y}-\mathbf{x})]^2 + \beta^2||\mathbf{y}-\mathbf{x}||^2}$$

with $\beta^2 = (1-\mathbf{M}\cdot\mathbf{M})$, and $\mathbf{M} = \mathbf{v}_{_B}/c_0$ denoting the body Mach number [27]. The symbol $[...]_\theta$ means evaluation at retarded time, $t-\theta$, where, for $\mathbf{x}$ and $\mathbf{y}$ fixed in the BFR, the acoustic time delay (namely, the time taken by a perturbation emitted in $\mathbf{y}$ to reach $\mathbf{x}$), θ, is given by [27]

$$c_0\theta = \hat{r} = \|\boldsymbol{\xi}_x - \boldsymbol{\xi}_y\| = \frac{1}{\beta^2}[r_\beta + \mathbf{M}\cdot(\mathbf{y}-\mathbf{x})] \quad (4)$$

Here $\boldsymbol{\xi}_x = \boldsymbol{\xi}(\mathbf{x},t)$ and $\boldsymbol{\xi}_y = \boldsymbol{\xi}(\mathbf{y},t-\theta)$ are the observer and source positions in the MFR, respectively at the current and retarded times. In addition,

$$\frac{\partial(\cdot)}{\partial \hat{n}} = \frac{\partial(\cdot)}{\partial n} - \mathbf{M}\cdot\mathbf{n}\,\mathbf{M}\cdot\nabla(\cdot)$$

with $\mathbf{n}$ denoting the body outward unit normal, and $\phi_i(\mathbf{x},t) = A_i(t-\theta)\,G(\mathbf{x},\mathbf{x}_i)$ represents the value of the incident velocity potential field generated by the perturbation source (note that, even though the integral scattering formulation is here developed considering an illustrative incident field due to a potential source, it remains valid for any incident field generated by any kind of flow perturbation).

Then, the velocity potential is decomposed as $\phi = \phi_{st} + \phi_i + \phi_s$, with ϕ_{st} denoting the velocity potential field associated to the flow perturbation generated by the uniform translation of the body (and hence steady in the BFR) and, ϕ_s representing the velocity potential scattered by the body as a response to the incident field, ϕ_i. It is possible to demonstrate that, assuming $\phi_s + \phi_i$ to be a

small perturbation with respect to ϕ_{st}, the scattered field solution may be obtained by the following linearized, frequency-domain, boundary-field integral equation (see Appendix B)

$$\begin{aligned}\tilde{\phi}_s(\mathbf{x},k) &= \int_{\mathcal{S}} \left[G\left(-\frac{\partial\tilde{\phi}_i}{\partial n} - \mathbf{M}\cdot\mathbf{n}\mathbf{M}\cdot\nabla\tilde{\phi}_s\right) - \tilde{\phi}_s\frac{\partial G}{\partial\hat{n}} + jk\,\tilde{\phi}_s\,G\left(\frac{\partial\hat{r}}{\partial\hat{n}} + 2\,\mathbf{M}\cdot\mathbf{n}\right)\right] e^{-jk\hat{r}}\,\mathrm{d}\mathcal{S}(\mathbf{y}) \\ &+ \int_{\mathcal{V}} G\;\tilde{\mu}\,e^{-jk\hat{r}}\,\mathrm{d}\mathcal{V}(\mathbf{y}) \end{aligned} \tag{5}$$

where $\tilde{(\cdot)}$ means Fourier transformation, $k = \omega/c_0$ is the wave number, and the fluctuating impermeability boundary condition $\partial\phi_s/\partial n = -\partial\phi_i/\partial n$ has been applied (the latter resulting from the overall impermeability boundary condition, $\partial\phi/\partial n = \mathbf{v}_B\cdot\mathbf{n}$, combined with the steady impermeability boundary condition, $\partial\phi_{st}/\partial n = \mathbf{v}_B\cdot\mathbf{n}$).

The field contribution, $\mu = \mu(\phi_{st},\phi_s,\phi_i)$, represents the first-order perturbation approximation of nonlinear terms about the value in the reference steady condition, $\sigma(\phi_{st})$, thereby linearly dependent on incident and scattered velocity potential. For $\phi_p = \phi_s + \phi_i$, $\mathbf{v}_{st} = \nabla\phi_{st}$ and $v_{st} = \|\mathbf{v}_{st}\|$, combining Eq. (2) with Bernoulli's theorem and tranforming into frequency domain, the following expression is derived (see Appendix A)

$$\tilde{\mu} = A_1\nabla^2\tilde{\phi}_p + jk\;A_2\;\tilde{\phi}_p + (\mathbf{A}_3 + jk\;\mathbf{A}_4)\cdot\nabla\tilde{\phi}_p + \mathbf{A}_5\cdot\nabla\left(\mathbf{v}_{st}\cdot\nabla\tilde{\phi}_p\right) \tag{6}$$

where the time-independent coefficients are given by

$$\begin{aligned} A_1 &= \frac{(\gamma-1)}{{c_0}^2}\left(\frac{{v_{st}}^2}{2} - \mathbf{v}_B\cdot\mathbf{v}_{st}\right); \quad A_2 = \frac{(\gamma-1)}{c_0}\,\nabla^2\phi_{st} \\ \mathbf{A}_3 &= \frac{1}{{c_0}^2}\left[\frac{\nabla{v_{st}}^2}{2} + (\gamma+1)\,(\mathbf{v}_{st} - \mathbf{v}_B)\,\nabla^2\phi_{st}\right] \\ \mathbf{A}_4 &= \frac{2}{c_0}\,\mathbf{v}_{st}; \quad \mathbf{A}_5 = \frac{1}{{c_0}^2}\,(\mathbf{v}_{st} - 2\,\mathbf{v}_B) \end{aligned} \tag{7}$$

Since resulting from a perturbation process about the steady reference condition, the linearized field contribution, μ, depends on the velocity potential ϕ_{st} (either through gradient or Laplacian operators): this means that (i) the application of the developed acoustic wave scattering formulation in Eq. (5) requires the prior solution of the aerodynamic field related to the scatterer motion, and (ii) the field sources tend to vanish with the increase of the distance from the body, as it occurs for the flow perturbation generated by the steady body motion. Equation (6) combined with the expressions in Eq. (7) is closely related to the linearized potential differential equation given in Ref. [23].

Note that, considering ϕ_{st} as the potential describing the non-uniform component of the mean flow in the BFR, it is possible to demonstrate that the contribution to $\tilde{\mu}$ defined by the coefficient $\mathbf{A}_4$ in Eq. (7) coincides with the non-uniform convective term of the weakly non-uniform, potential flow wave equation, governing the scattering approaches in Refs. [15]-[20]. Therefore, the proposed formulation may be considered as an extension of the widely-applied nonuniform potential flow approaches for the analysis of moving-body sound scattering.

B. Discretization of the integral formulation

For the numerical solution of the integral formulation introduced, Eq. (5) is discretized by a zero-th order boundary-field element method, for which the body surface, $\mathcal{S}$, and the field domain of interest, $\mathcal{V}$, are divided into M quadrilateral panels and Q six-face volumes (derived from H-grid or C-grid meshes, depending on the shape of the body), respectively. Then, assuming the velocity potential and its gradient uniformly distributed within the elements of discretization with values equal to those at the centroids of the elements, and evaluating Eq. (5) at each of these centroids (thus, using it as a boundary-field integral equation), a set of $M+Q$ algebraic equations is obtained

$$\begin{bmatrix} \mathbf{C}^{SS} & \mathbf{C}^{SV} \\ \mathbf{C}^{VS} & \mathbf{C}^{VV} \end{bmatrix} \begin{Bmatrix} \tilde{\boldsymbol{\phi}}_s^S \\ \tilde{\boldsymbol{\phi}}_s^V \end{Bmatrix} = \begin{bmatrix} \mathbf{B}^{SS} & \mathbf{B}^{SV} \\ \mathbf{B}^{VS} & \mathbf{B}^{VV} \end{bmatrix} \begin{Bmatrix} \tilde{\boldsymbol{\phi}}_i^S \\ \tilde{\boldsymbol{\phi}}_i^V \end{Bmatrix} \tag{8}$$

where $\boldsymbol{\phi}_s^S$ and $\boldsymbol{\phi}_s^V$ denote the vectors collecting the unknown scattered potential at the centroids of the body surface boundary elements and at the centroids of the volumes surrounding the body, respectively, whilst $\boldsymbol{\phi}_i^S$ and $\boldsymbol{\phi}_i^V$ are the vectors of the incident potential evaluated at the same sets of centroids.

Matrices $\mathbf{C}^{SS}, \mathbf{C}^{SV}, \mathbf{B}^{SS}, \mathbf{B}^{SV}$ collect the influence coefficients from surface and volume elements to surface centroids, while $\mathbf{C}^{VS}, \mathbf{C}^{VV}, \mathbf{B}^{VS}, \mathbf{B}^{VV}$ are the matrices of the influence coefficients from surface and volume elements to volume centroids.

Once Eq. (8) is solved, the scattered sound in the field may be readily evaluated by using Eq. (5) as an integral representation, followed by application of the Bernoulli theorem which, for far-field small perturbations of homentropic flows, in the BFR yields

$$p_s = -\rho_0 \left(\frac{\partial \phi_s}{\partial t} - \mathbf{v}_{_B} \cdot \nabla \phi_s \right) \tag{9}$$

Finally, note that a drawback in using an integral method like that presented here is the possible presence of nonphysical (spurious) characteristic frequencies in the resulting integral equation, which can completely destroy the corresponding numerical solution. In our case, these correspond to the eigenvalues of the Dirichlet interior problem and depend on the shape of the scatterer [24]. This problem might be overcome by using the CHIEF regularization technique introduced in Ref. [25], that consists of augmenting the set of equations of the discretized integral operator with homogeneous condition equations at some points in the interior domain, followed by the application of a least-squares technique for the computation of unknowns (see, for instance, Ref. [26]). Should spurious resonance problems arise, the CHIEF regularization technique might directly be applied to the proposed formulation.

III. NUMERICAL RESULTS

Numerical investigations are aimed at assessing both the influence of the linearized field terms included in the proposed novel integral approach and the discrepancies among the predictions provided by the fully-linear VP, LE and FWHE formulations (namely, those formulations obtained by totally neglecting the field terms). For the sake of clarity and a better understanding of the results discussed in the following, a brief outline of the LE and FWHE formulations considered in this work is provided in Appendix C.

The scattering problem examined consists of a rectangular nonlifting wing in uniform rectilinear translation, with incident harmonic potential field generated by a co-moving point source, located in the mid-span plane [22]. The span of the wing, $2L$, is three times the chord length, c_w, and two different cross section shapes are investigated, namely a symmetric biconvex parabolic airfoil with thickness ratio $t_w/c_w = 0.1$ and a NACA 0012 airfoil.

For $\mathcal{R}(\mathbf{x}_c, x, y, z)$ denoting a wing-fixed coordinate system having chordwise x-axis, spanwise y-axis and origin, $\mathbf{x}_c$, at the centre of the mid-span cross section (see Fig. 1), the acoustic scattering predictions are presented in terms of directivity patterns of the ratio between the scattered pressure and a reference pressure defined as $p_{ref} = 2\,d\,|\tilde{p}_i(\mathbf{x}_c, k)|/c_w$ [22] evaluated in the mid-span plane, at radial distance $d/c_w = 52.5$ from $\mathbf{x}_c$, with the wing moving in the negative x-axis direction. As

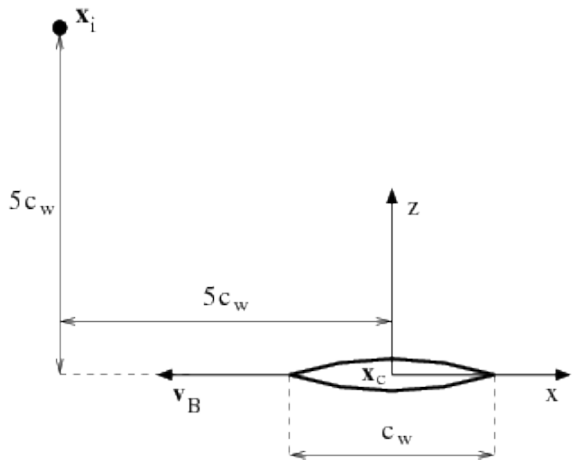

Fig. 1 Mid-plane of the scattering wing. Wing velocity and location of point source.

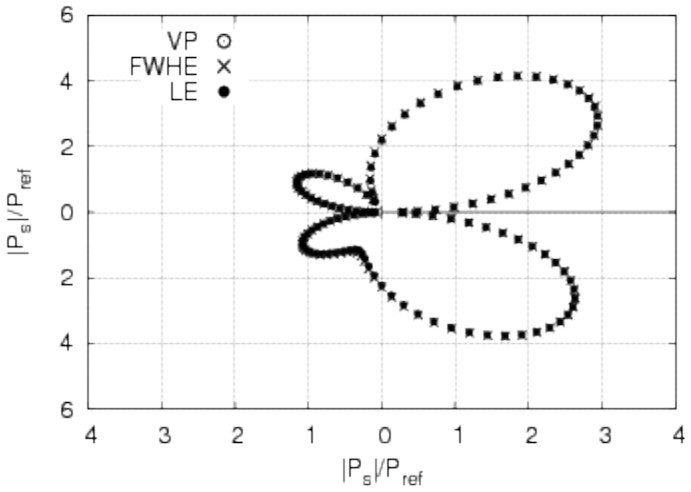

Fig. 2 Noise directivity pattern for $M = 0$ and $k\,c_w = 6$. Biconvex parabolic airfoil wing, fully-linear formulations.

depicted in Fig. 1, the perturbation source generating the incident potential field is located in front of the wing at $\mathbf{x}_i = (-5c_w, 0, 5c_w)$.

First, figures 2 and 3 show the comparisons among the predictions given by the fully-linear VP, LE and FWHE formulations, respectively for the biconvex parabolic airfoil wing and for the NACA 0012 airfoil wing, when the body is at rest and the wave number of the incident perturbation signal is such that $k\,c_w = 6$ (note that, the numerical results are obtained by the biconvex parabolic airfoil

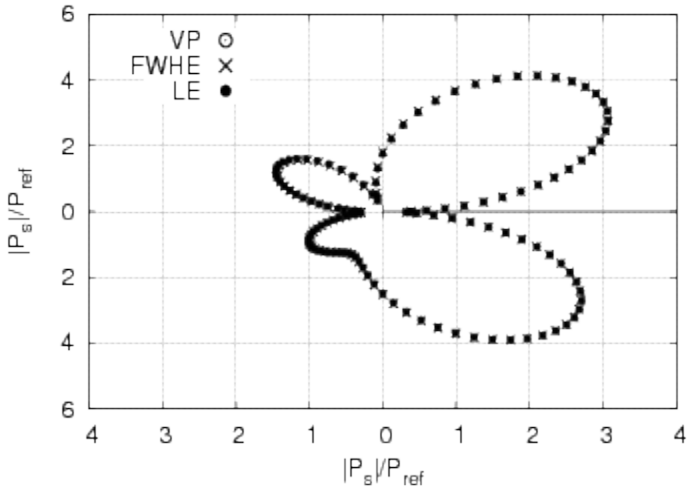

Fig. 3 Noise directivity pattern for $M = 0$ and $k\,c_w = 6$. NACA 0012 airfoil wing, fully-linear formulations.

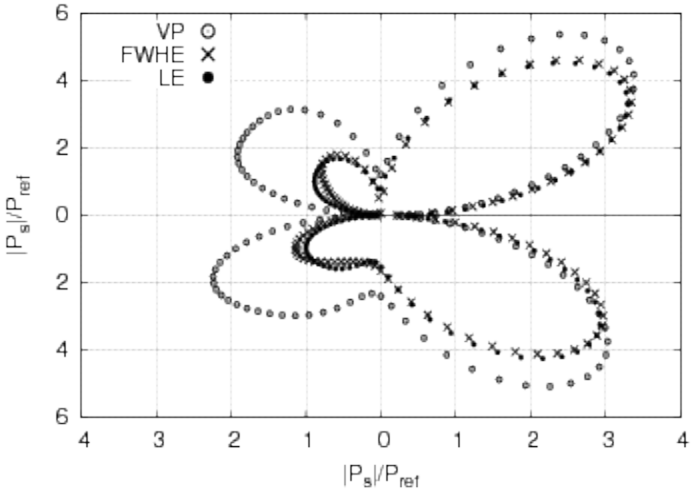

Fig. 4 Noise directivity pattern for $M = 0.5$ and $k\,c_w = 6$. Biconvex parabolic airfoil wing, fully-linear formulations.

wing surface discretized into 2304 panels and the NACA 0012 wing surface discretized into 3072 panels, as indicated by dedicated convergence analyses, see later). These figures demonstrate that the three fully-linear formulations considered provide results that are perfectly equivalent when the scatterer is fixed with respect to the unperturbed fluid. Similar observations can be made for the results obtained for $k\,c_w = 10$, not shown here for the sake of conciseness.

However, the fully-linear VP, LE and FWHE formulations show discrepancies when the scatterer is moving at Mach number $M = 0.5$ for both cross-section shapes examined. This is shown in figures

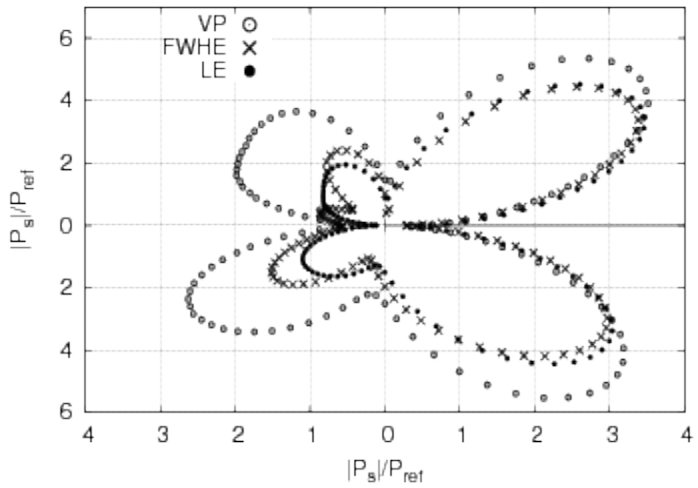

Fig. 5 Noise directivity pattern for $M = 0.5$ and $k\,c_w = 6$. NACA 0012 airfoil wing, fully-linear formulations.

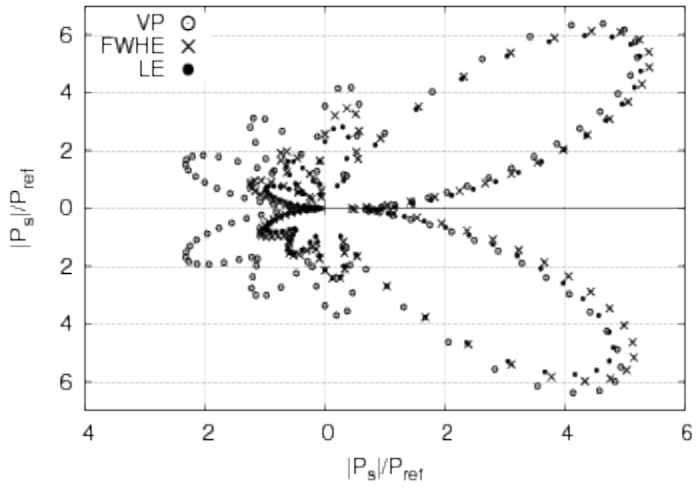

Fig. 6 Noise directivity pattern for $M = 0.5$ and $k\,c_w = 10$. Biconvex parabolic airfoil wing, fully-linear formulations.

4 and 5 for $k\,c_w = 6$, and in figures 6 and 7 for $k\,c_w = 10$. Specifically, LE and FWHE formulations provide similar results for the biconvex parabolic airfoil wing but, although the Mach number is not particularly high and even for the scatterer with low-curvature surface (see figures 4 and 6), the differences between LE and FWHE predictions and those obtained by the VP approach are appreciable (note that, the VP predictions are in perfect agreement with those obtained in Ref. [22] through an equivalent linear velocity potential approach).

It is worth observing that, the Neumann boundary conditions might be obtained from a lin-

earized form of the Euler equation for the moving body. Nonetheless, in that case, the LE solution would be dependent on that given by the VP formulation (see Appendix C, Eq. (C.5)), thus affected by its inaccuracies. For this reason, in order to compare the intrinsic relative accuracy among the examined formulations, the LE results presented in figures 4-7 are obtained by deriving the Neumann boundary conditions from the widely-used linear homogeneous condition $\partial p/\partial n = 0$ (namely, the linearized condition holding for non-moving bodies, see Eq. (C.5)). For $M = 0.5$ and $k\,c_w = 6$, figure 8 shows the effect on the LE solution of the introduction of boundary conditions given by the linearized form of the Euler equation: for the biconvex parabolic airfoil wing linear and linearized boundary conditions provide very similar results, whereas wider differences appear for the NACA 0012 airfoil wing case, particularly in the region more influenced by the leading edge (similar conclusions may be drawn also for $k\,c_w = 10$, as indicated by a numerical investigation not shown here for the sake of conciseness). Figure 8(b) demonstrates that the inclusion of linearized boundary condition terms makes LE predictions closer to FWH ones, especially in the region more affected by the leading edge scattering.

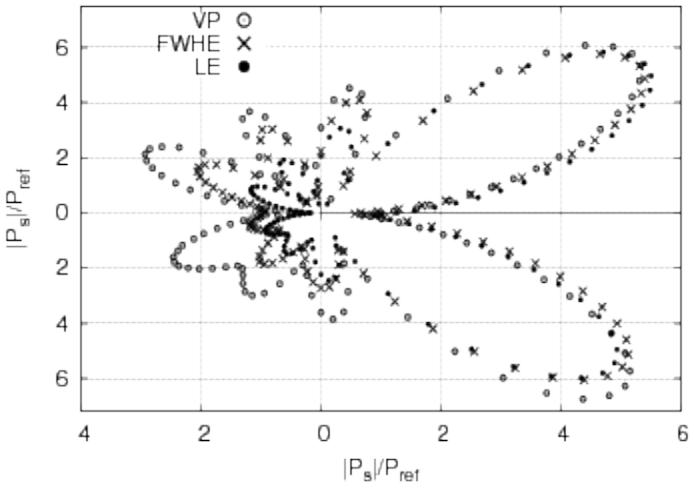

Fig. 7 Noise directivity pattern for $M = 0.5$ and $k\,c_w = 10$. NACA 0012 airfoil wing, fully-linear formulations.

Observing that the results from the three formulations considered are based on the same potential-flow modeling assumptions, the differences observed for the moving scatterer are necessarily due to the different importance of the nonlinear terms that are neglected in fully-linear

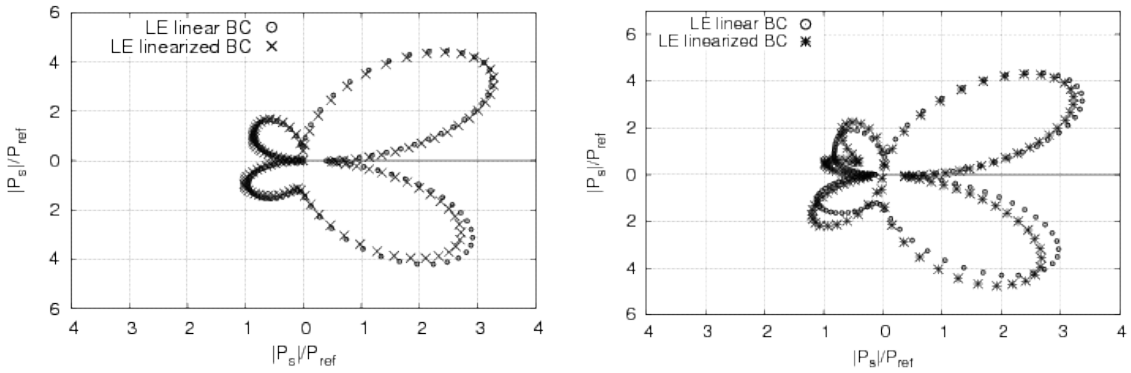

(a) biconvex-airfoil wing

(b) NACA 0012-airfoil wing

Fig. 8 Noise directivity pattern for $M = 0.5$ and $k\,c_w = 6$. Effect of boundary conditions on fully-linear LE approach.

formulations. Hence, the proposed novel VP linearized formulation is applied to the scattering problems considered in order to quantify the relevance of the nonlinear field contributions.

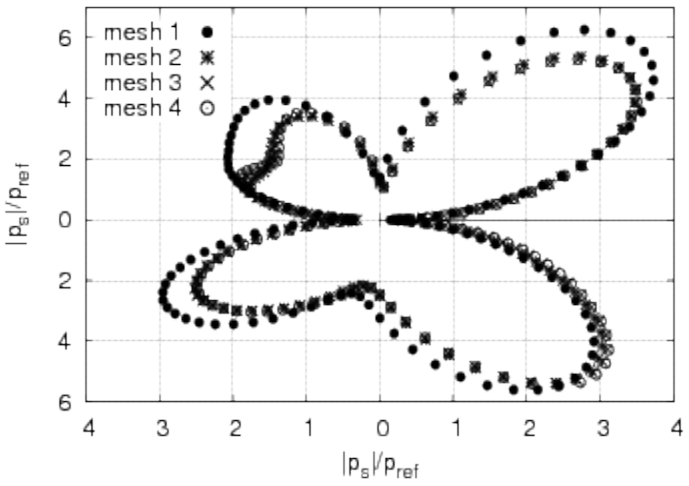

Fig. 9 Noise directivity convergence analysis for $M = 0.5$ and $k\,c_w = 6$. NACA 0012 airfoil wing.

The results presented in the following are obtained considering the extension of the field volume, $\mathcal{V}$, in Eq. (5) and wing/volume discretization meshes as those determined through a previous convergence analysis of the numerical solution.

For instance, figure 9 presents the convergence analysis of the noise scattering predictions concerning the NACA 0012 airfoil wing, $M = 0.5$, $k\,c_w = 6$ case, for the mesh discretization refinement

and external volume size increase reported in table 1. It is apparent that the results obtained by *mesh 4* showing a percentage rms relative error (rms-re) equal to 2.5% may be considered to be converged (rms-re is defined as the difference of the predictions determined by *mesh n* and *mesh n-1* divided by the predictions determined by *mesh n-1*). Hence, as resulting from the convergence

Table 1 Mesh discretization convergence analysis; NACA 0012 airfoil wing, $M = 0.5$**,** $k\,c_w = 6$**.**

	surface panels	volume panels	volume extension	rms-re
mesh 1	420	1800	$0.6\,c_w$	—
mesh 2	1232	10560	$0.8\,c_w$	15%
mesh 3	2436	31320	$1.0\,c_w$	4%
mesh 4	4032	69120	$1.2\,c_w$	2.5%

analyses carried out for the considered scattering configurations, when $M = 0.5$, for the biconvex parabolic airfoil wing case, 2304 panels are used on the surface, whereas the field domain $\mathcal{V}$ is discretized by 40960 volume elements (parallelepipeds derived from a H-grid mesh), with the distance of its external boundary from the surface equal to the $0.8\,c_w$; for the NACA 0012 airfoil wing, the panels used on the surface are 4032 for $k\,c_w = 6$ and 7680 for $k\,c_w = 10$, the distance of the external boundary of $\mathcal{V}$ from the surface is equal to $1.2\,c_w$, while, using a C-grid mesh, 69120 and 132288 discretization volume elements are used, respectively, for $k\,c_w = 6$ and $k\,c_w = 10$. Note that, a similar convergence analysis has been accomplished for the evaluation of the steady aerodynamic solution affecting the linearized field terms in Eq. (5).

Figures 10 and 11 show the scattered potential evaluated on two sections of the biconvex parabolic airfoil and NACA 0012 airfoil wings, respectively, for $M = 0.5$ and $k\,c_w = 6$. Specifically, predictions from the boundary-field VP formulation compared with those from the fully-linear one at the sections located at $y/L = 0.3$ and $y/L = 0.8$, demonstrate that the solution is affected by the nonlinear terms throughout the whole chord length, with greater differences appearing in the high-curvature, leading-edge region of the NACA 0012 airfoil scatterer, where the gradient of the steady reference potential in the field coefficients of Eq. (7) becomes significant. This is shown in figure 12, which plots the ϕ_{st} distribution evaluated on the biconvex parabolic and NACA 0012 airfoil wings, where the sharp gradient near the leading edge of the NACA 0012 wing is evident.

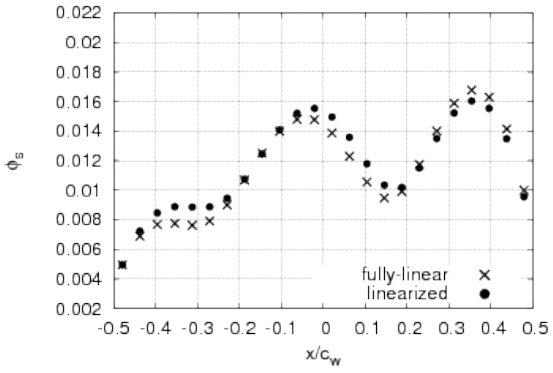

(a) $y/L = 0.3$

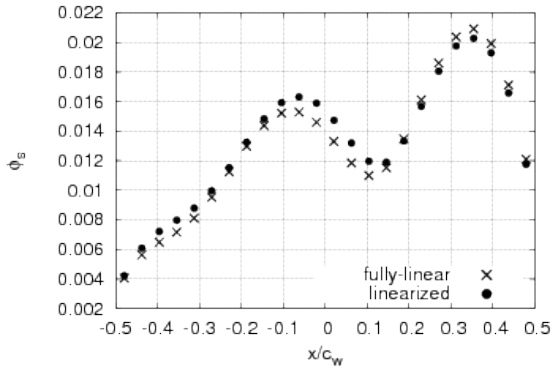

(b) $y/L = 0.8$

Fig. 10 Magnitude of scattered potential on the biconvex parabolic airfoil wing from VP formulations

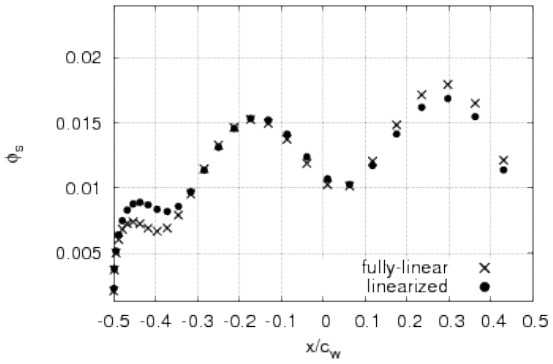

(a) $y/L = 0.3$

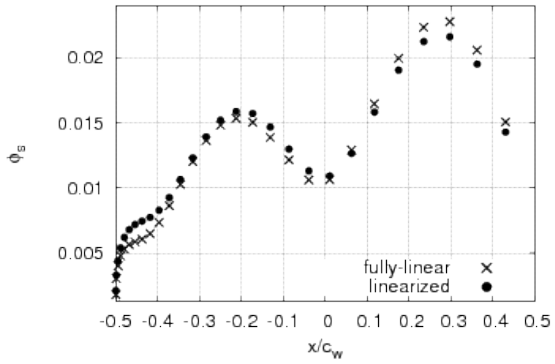

(b) $y/L = 0.8$

Fig. 11 Magnitude of scattered potential on the NACA 0012 airfoil wing from VP formulations.

Minor variations in the spanwise distributions of ϕ_{st} are noted. It is worth mentioning that it is determined from the full compressible-flow equation through solution of Eq. (3), with $\phi \equiv \phi_{st}, \phi_i = 0$ and $\partial\phi_{st}/\partial n = \mathbf{v}_B \cdot \mathbf{n}$.

Next, the effect of the scatterer velocity on the introduced linearized field terms is examined. Figures 13 and 14 depict the comparison between fully-linear and linearized scattered pressure predictions concerning the two examined wings with $k\, c_w = 6$, at $M = 0.3$ and $M = 0.5$, respectively. For both scatterers, the fully-linear formulation provides satisfactory simulations when $M = 0.3$, but notable influence of the field terms on the directivity patterns is clearly observed for $M = 0.5$, particularly at the microphones placed in the front region. As noted above for figures 10 and 11,

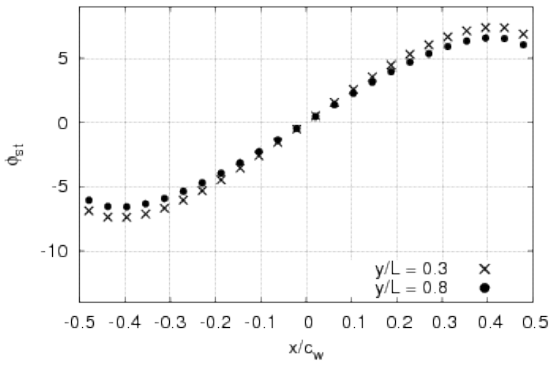

(a) biconvex-airfoil wing

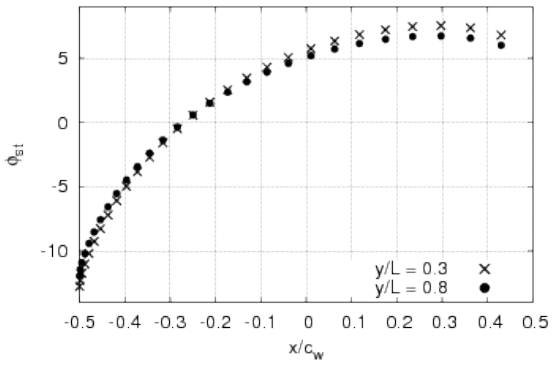

(b) NACA 0012-airfoil wing

Fig. 12 Steady reference potential for $M = 0.5$.

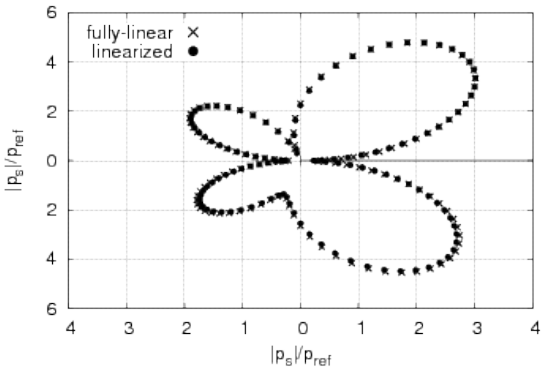

(a) $M = 0.3$

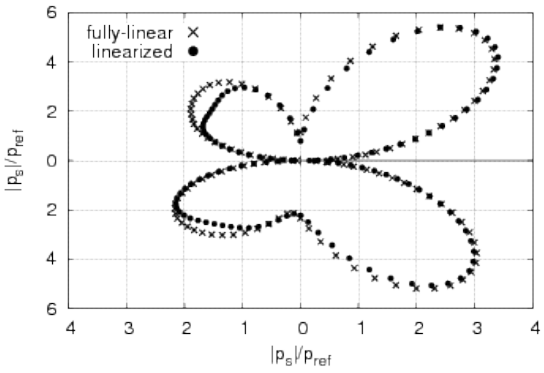

(b) $M = 0.5$

Fig. 13 Noise directivity pattern by VP formulations. Biconvex parabolic airfoil wing, $k\,c_w = 6$.

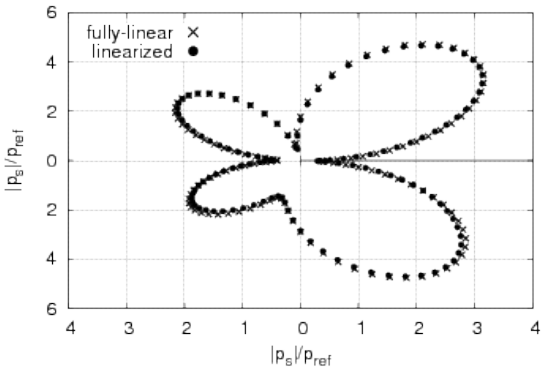

(a) $M = 0.3$

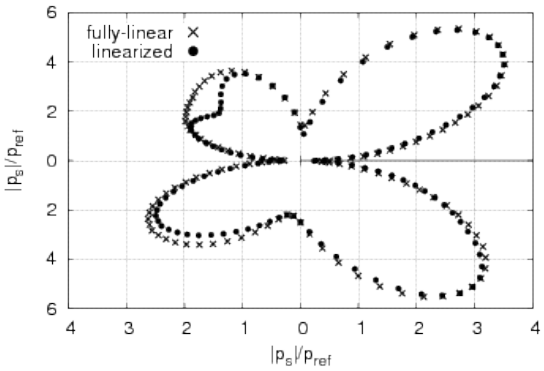

(b) $M = 0.5$

Fig. 14 Noise directivity pattern by VP formulations. NACA 0012 airfoil wing, $k\,c_w = 6$.

this result is a direct consequence of the fact that the field term coefficients of Eq. (7) are strongly dependent on the gradient of the steady velocity potential; for this reason, it is also expected that

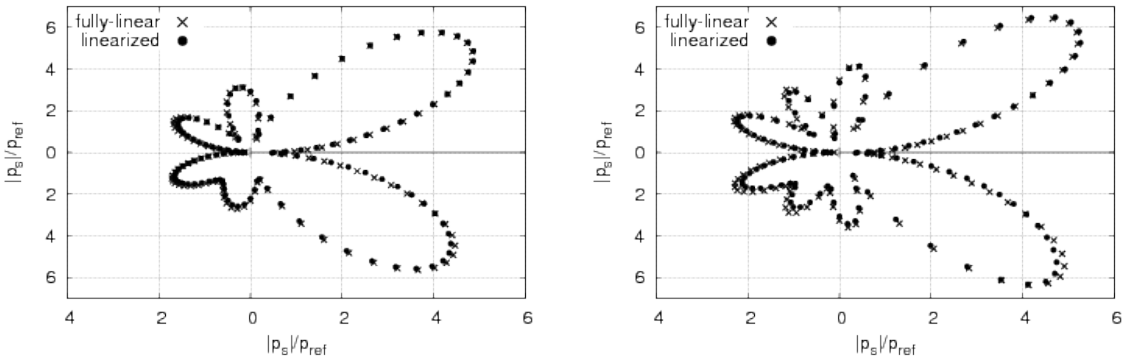

(a) $M = 0.3$ (b) $M = 0.5$

Fig. 15 Noise directivity pattern by VP formulations. Biconvex parabolic airfoil wing, $kc_w = 10$.

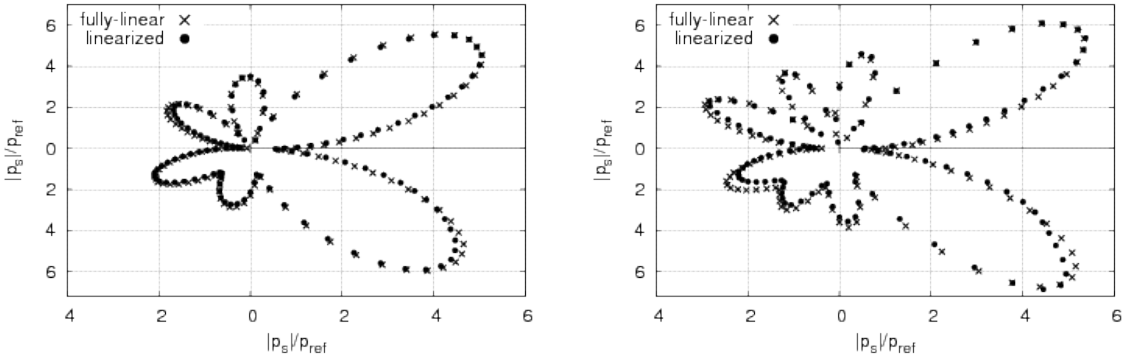

(a) $M = 0.3$ (b) $M = 0.5$

Fig. 16 Noise directivity pattern by VP formulations. NACA 0012 airfoil wing, $k\,c_w = 10$.

for lifting wings at non-zero angle of attack, non-negligible nonlinear effects would start appearing at lower scatterer velocities.

Similar considerations are appropriate for the results shown in figures 15 and 16 and concerning the same analysis for the incident perturbation signal with $k\,c_w = 10$. In this case, however, in addition to a multi-lobe directivity pattern, it is observed that the contribution of the linearized field terms of the VP formulation is less relevant than for $k\,c_w = 6$.

Finally, for the biconvex parabolic airfoil wing moving at $M = 0.5$, figures 17 and 18 show, respectively for $k\,c_w = 6$ and $k\,c_w = 10$, the direct comparisons of the scattered directivity patterns predicted by the proposed boundary-field VP integral approach with those provided by VP, LE and FWHE fully-linear formulations. Equivalent comparisons are presented in figures 19 and 20 for the scattering NACA 0012 airfoil wing moving at $M = 0.5$. Two considerations may be drawn from

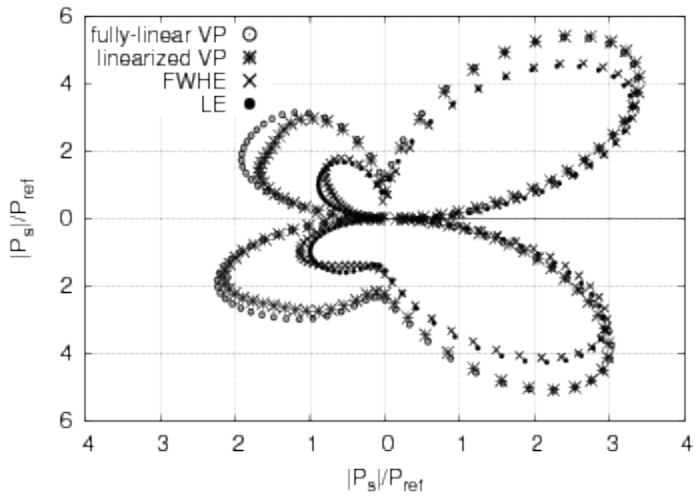

Fig. 17 Noise directivity pattern from the biconvex parabolic airfoil wing. Comparison among fully-linear and linearized formulations for $M = 0.5$ and $k\,c_w = 6$.

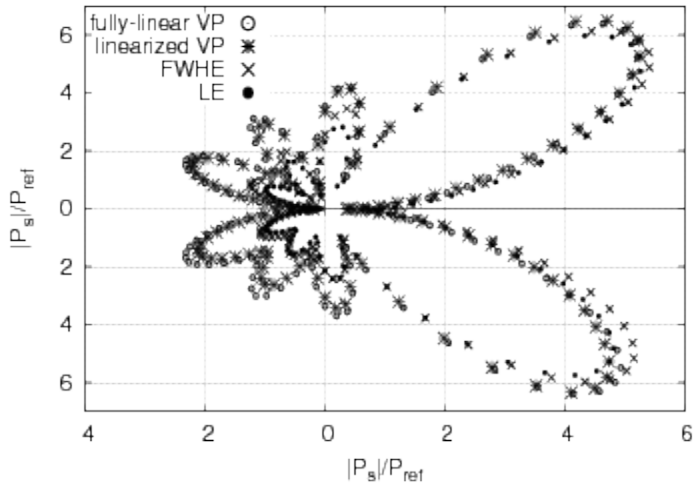

Fig. 18 Noise directivity pattern from the biconvex parabolic airfoil wing. Comparison among fully-linear and linearized formulations for $M = 0.5$ and $k\,c_w = 10$.

these results: firstly, the effect of the linearized field terms is to make VP predictions closer to those provided by the pressure-based formulations considered (and this trend is encouraging in view of the expected matching of all predictions, once linearized field terms are included in all formulations); secondly, at least for the configurations examined here, the predictions from the fully-linear VP formulation are evidently closer to the noise directivity patterns given by the approach including the linearized boundary-field terms, than those provided by the LE and FWHE, pressure-based, fully-linear formulations.

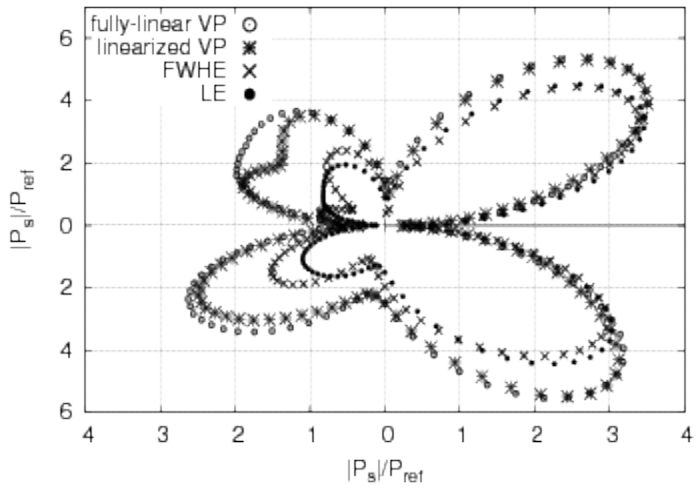

Fig. 19 Noise directivity pattern from the NACA 0012 airfoil wing. Comparison among fully-linear and linearized formulations for $M = 0.5$ and $k\,c_w = 6$.

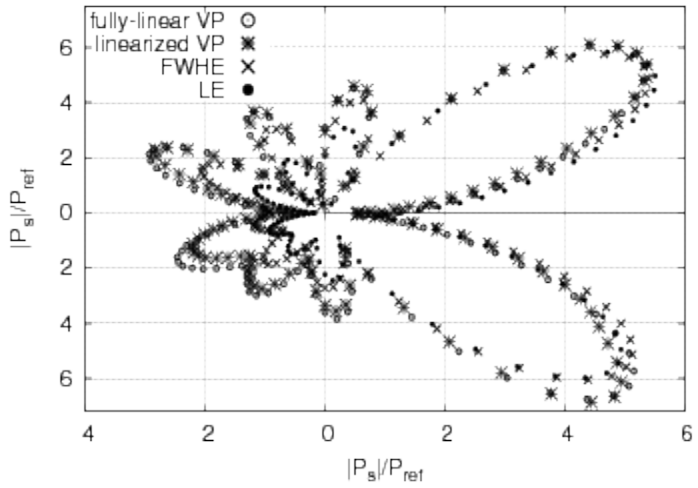

Fig. 20 Noise directivity pattern from the NACA 0012 airfoil wing. Comparison among fully-linear and linearized formulations for $M = 0.5$ and $k\,c_w = 10$.

Note that, the optimization of the numerical tool performance being out of the scope of this work, all of the linearized VP results have been obtained by solving Eq. (8) through a standard LU decomposition algorithm (a computational cost of a couple of hours is required for the finer mesh on a common desktop PC).

IV. Conclusions

A novel boundary-field integral velocity potential formulation for the prediction of noise scattered by moving bodies has been developed and verified. It includes field terms suitably linearized about a reference steady motion condition, which vanish for fixed scatterers and take into account the effects of nonuniform mean flow, without introducing the low Mach number or weakly nonuniform flow assumptions considered in widely-applied scattering formulations for moving bodies. A nonlifting rectangular wing translating at uniform velocity, impinged by a perturbation wave emitted by a co-moving pulsating source has been examined. Linear integral formulations for sound scattering based on Lighthill and Ffowcs-Williams and Hawkings equations have been also considered for comparison. The main outcomes of the accomplished analyses are the following:

- the noise scattering predictions obtained by VP, LE and FWHE fully-linear integral formulations perfectly match for fixed scatterers, but present growing discrepancies with the increase of the scatterer velocity;
- the inclusion of the linearized field terms in the VP formulation may produce significant modification of the predicted scattered noise, depending on the velocity and shape of the scattering body and on the wave number of the perturbation signal: larger field term effects are present where the shape of the scatterer induces relevant gradients of the velocity potential associated to the unperturbed steady condition of the scatterer;
- the inclusion of the linearized field terms moves VP formulation results closer to the predictions provided by the pressure-based fully-linear formulations;
- however, the predictions from the boundary-field approach are evidently closer to the results given by the fully-linear VP formulation, than to those provided by the LE and FWHE fully-linear formulations: this proves that the VP formulation yields the most accurate fully-linear solver for the analysis of sound scattered by moving bodies.

The VP, LE and FWHE frequency-domain integral formulations presented in this work are formally identically valid also for rigid scatterers subject to uniform rotation or uniform rotation combined with uniform axial translation, with suited expressions of Green's function and time delay.

APPENDIX A: EXTRACTION OF LINEAR FIELD CONTRIBUTION

Assuming the potential field decomposed into steady and perturbation components, $\phi = \phi_{st} + \phi_p$, with $\phi_p = \phi_i + \phi_s$, for $\mathbf{v}_{st} = \nabla\phi_{st}$, $\mathbf{v}_p = \nabla\phi_p$, $v = \|\mathbf{v}\|, v_{st} = \|\mathbf{v}_{st}\|, v_p = \|\mathbf{v}_p\|$, and observing that:

- from Bernoulli's theorem expressed in the BFR [27, 28]

$$1 - \frac{c^2}{{c_0}^2} = \frac{\gamma - 1}{{c_0}^2}\left(\frac{\partial\phi}{\partial t} - \mathbf{v}_{_B}\cdot\nabla\phi + \frac{v^2}{2}\right)$$

  with $v^2 = {v_{st}}^2 + {v_p}^2 + 2\,\mathbf{v}_{st}\cdot\mathbf{v}_p$

- $$\frac{\partial v^2}{\partial t} - \mathbf{v}_{_B}\cdot\nabla v^2 = -\mathbf{v}_{_B}\cdot\nabla {v_{st}}^2 + \frac{\partial v_p^2}{\partial t} - \mathbf{v}_{_B}\cdot\nabla v_p^2 + 2\left[\mathbf{v}_{st}\cdot\frac{\partial\mathbf{v}_p}{\partial t} - \mathbf{v}_{_B}\cdot\nabla(\mathbf{v}_{st}\cdot\mathbf{v}_p)\right]$$

- $$\mathbf{v}\cdot\nabla v^2 = \mathbf{v}_{st}\cdot\nabla {v_{st}}^2 + \mathbf{v}_p\cdot\nabla v_p^2 + 2\,\mathbf{v}_{st}\cdot\nabla(\mathbf{v}_{st}\cdot\mathbf{v}_p) + \mathbf{v}_p\cdot\nabla {v_{st}}^2 + \mathcal{O}(v_p^2)$$

the combination of Eq. (2) with the above equations yields

$$\sigma(\phi) = \sigma(\phi_{st}) + \sigma(\phi_i) + \mu(\phi_{st}, \phi_p) + \mathcal{O}(\phi_p^2) \tag{A.1}$$

with μ linearly dependent on the perturbation velocity potential and given by the expression in Eq. (6), once transformed into frequency domain.

APPENDIX B: INTEGRAL FORMULATION FOR THE SCATTERED FIELD

The potential field, ϕ_{st}, denotes the steady solution for the problem of the nonlifting body in uniform translation in the absence of the perturbing source and, therefore, satisfies the following time-independent integral representation

$$\phi_{st}(\mathbf{x}) = \int_{\mathcal{S}}\left[G\frac{\partial\phi}{\partial\hat{n}} - \phi\frac{\partial G}{\partial\hat{n}}\right]\mathrm{d}\mathcal{S}(\mathbf{y}) + \int_{\mathcal{V}} G\left[\sigma(\phi_{st})\right]\mathrm{d}\mathcal{V}(\mathbf{y}) \tag{B.1}$$

where $\sigma(\phi_{st})$ are the nonlinear terms related to the steady potential solution.

At the same time, considering the presence of the perturbation source of intensity, $A_i(t)$, at the point $\mathbf{x}_i$, in the absence of the scattering body, for a fictitious (and hence permeable) surface, $\mathcal{S}_f \equiv \mathcal{S}$, the following integral representation may be derived by applying the boundary integral approach to the fluid volume external to $\mathcal{S}_f$ [14, 27]

$$\phi_i(\mathbf{x},t) = \int_{\mathcal{S}_f}\left[G\frac{\partial\phi_i}{\partial\hat{n}} - \phi_i\frac{\partial G}{\partial\hat{n}} + \frac{\partial\phi_i}{\partial t}\,G\left(\frac{\partial\theta}{\partial\hat{n}} + 2\frac{\mathbf{M}\cdot\mathbf{n}}{c_0}\right)\right]_\theta \mathrm{d}\mathcal{S}(\mathbf{y}) + \int_{\mathcal{V}} G\left[\sigma(\phi_i)\right]_\theta \mathrm{d}\mathcal{V}(\mathbf{y}) + \phi_i(\mathbf{x},t) \tag{B.2}$$

with $\sigma(\phi_i)$ denoting the nonlinear terms related to the incident potential. Equation (B.2) demonstrates that wherever in the field, the integral contribution of the incident potential vanishes whatever the fluid boundaries considered.

Then, for $\phi = \phi_{st} + \phi_i + \phi_s$, subtracting Eqs. (B.1) and (B.2) from Eq. (3), combining with Eq. (A.1) and neglecting second-order perturbation terms, $\mathcal{O}(\phi_p^2)$, yields the following linear boundary-field integral representation for the scattered field

$$\phi_s(\mathbf{x},t)=\int_{\mathcal{S}}\left[G\frac{\partial\phi_s}{\partial\hat{n}}-\phi_s\frac{\partial G}{\partial\hat{n}}+\frac{\partial\phi_s}{\partial t}\,G\left(\frac{\partial\theta}{\partial\hat{n}}+2\frac{\mathbf{M}\cdot\mathbf{n}}{c_0}\right)\right]_\theta \mathrm{d}\mathcal{S}(\mathbf{y})+\int_{\mathcal{V}} G\left[\mu(\phi_{st},\phi_i,\phi_s)\right]_\theta \mathrm{d}\mathcal{V}(\mathbf{y}) \quad \text{(B.3)}$$

Next, observing that for $\mathbf{x}$ and $\mathbf{y}$ fixed in the BFR and under rigid-body assumption, all terms in Eq. (B.3) are time-constant except for ϕ_i and ϕ_s, and reminding that the Fourier transform, $\mathcal{F}$, of time-derived or time-delayed function, f, gives

$$\mathcal{F}\left[\frac{\partial f(t)}{\partial t}\right]=j\omega\,\tilde{f}(\omega) \quad \text{and} \quad \mathcal{F}\left[f(t-\tau)\right]=\tilde{f}(\omega)\,e^{-j\omega\tau}$$

with the imaginary angular frequency $j\omega$ denoting the Fourier variable, and $\tilde{f}(\omega)=\mathcal{F}[f(t)]$, the frequency-domain transformation of Eq. (B.3) yields

$$\tilde{\phi}_s(\mathbf{x},\omega)=\int_{\mathcal{S}}\left[G\frac{\partial\tilde{\phi}_s}{\partial\hat{n}}-\tilde{\phi}_s\frac{\partial G}{\partial\hat{n}}+j\omega\;\tilde{\phi}_s\,G\left(\frac{\partial\theta}{\partial\hat{n}}+2\frac{\mathbf{M}\cdot\mathbf{n}}{c_0}\right)\right]e^{-j\omega\theta}\,\mathrm{d}\mathcal{S}(\mathbf{y})+\int_{\mathcal{V}} G\,\tilde{\mu}\,e^{-j\omega\theta}\,\mathrm{d}\mathcal{V}(\mathbf{y}) \quad \text{(B.4)}$$

Finally, imposing the impermeability boundary conditions and replacing the angular frequency ω with the wave number $k=\omega/c_0$, the frequency-domain, boundary-field integral representation of the scattered field expressed in Eq. (5) is readily obtained.

APPENDIX C: LE AND FWHE FORMULATIONS FOR THE SCATTERED FIELD

Let us consider a body $\mathcal{B}$ in motion within a uniform medium, whose dynamics is governed by continuity and momentum equations (Euler equation for inviscid fluids, Navier-Stokes equation for viscous fluids). In the absence of sources of matter or external forces, in a MFR these equations are combined to derive the following Lighthill equation for the propagation of the acoustic pressure, $p'={c_0}^2(\rho-\rho_0)$, in the fluid domain [14, 29]

$$\Box^2 p'=\frac{1}{{c_0}^2}\frac{\partial^2 p'}{\partial t^2}-\nabla^2 p'=\nabla\cdot(\nabla\cdot\mathbf{T}), \qquad \boldsymbol{\xi}\in\mathbb{R}^3\backslash\mathcal{B} \quad \text{(C.1)}$$

where $\boldsymbol{\xi}$ denotes the position of a point in the MFR, $\mathbf{T} = (\hat{p} - p')\mathbf{I} + \rho\,\mathbf{v}\otimes\mathbf{v} - \mathbf{V}$ is the Lighthill stress tensor with $\mathbf{V}$ and $\hat{p}$ representing, respectively, the viscous stress tensor (neglected under inviscid fluid assumption) and the gauge pressure.

Next, defining the surface of the moving body by the function $f(\boldsymbol{\xi}, t) = 0$, with $f < 0$ inside of it and $f > 0$ outside, the generalized function, $\bar{p}' = H(f)\,p'$, is introduced, where $H(f)$ denotes the Heaviside unit function. Noting that $\nabla H(f) = \delta(f)\,\nabla f$, and assuming $\|\nabla f\| = 1$ and hence $\nabla f = \mathbf{n}$, the forcing term related to the field stresses in Eq. (C.1) can be expressed as

$$H\nabla\cdot(\nabla\cdot\mathbf{T}) = \nabla\cdot[\nabla\cdot(H\,\mathbf{T})] - \delta(f)\,\mathbf{n}\cdot(\nabla\cdot\mathbf{T}) - \nabla\cdot[\delta(f)\,\mathbf{T}\,\mathbf{n}] \tag{C.2}$$

Thus, using Eq. (C.2) in Eq. (C.1) rewritten for $\bar{p}'$ and combining with the continuity and the momentum equations yields the following Ffowcs-Williams and Hawkings equation for the acoustic pressure propagation [14, 30]

$$\Box^2\bar{p}' = \nabla\cdot[\nabla\cdot(H(f)\,\mathbf{T})] + \frac{\partial}{\partial t}\left[\rho_0\,\mathbf{v}_{_B}\cdot\mathbf{n}\,\delta(f)\right] - \nabla\cdot[\hat{p}\,\mathbf{n}\,\delta(f)]\,, \quad \boldsymbol{\xi}\in\mathbb{R}^3 \tag{C.3}$$

when the body impermeability conditions is applied ($\mathbf{v}\cdot\mathbf{n} = \mathbf{v}_{_B}\cdot\mathbf{n}$).

In the presence of an incident fluctuating acoustic pressure field, p'_i, radiated by independent sources of noise (for instance, the potential source, A_i, considered in Section II), LE and FWHE integral formulations for the sound scattered by the immersed body in uniform translation may be developed starting from Eq. (C.1) and Eq. (C.3), respectively.

LE formulation. Observing the similarity between the differential operators in Eq. (1) and (C.1) (the convective term in the wave operator of Eq. (1) takes into account the transformation of the time derivative from MFR to BFR), the same procedure based on the integral equation method used to solve Eq. (1) is applied also to integrate Eq. (C.1) (see Section II and Appendix B).

Thus, neglecting the linearized contribution that would derive from the field stresses, $\nabla\cdot(\nabla\cdot\mathbf{T})$, the following frequency-domain, fully-linear LE scattering boundary integral equation formulation in the BFR is readily derived

$$\tilde{p}'_s(\mathbf{x},k) = \int_{\mathcal{S}}\left[G\left(\frac{\partial\tilde{p}'_s}{\partial n} - \mathbf{M}\cdot\mathbf{n}\mathbf{M}\cdot\nabla\tilde{p}'_s\right) - \tilde{p}'_s\frac{\partial G}{\partial\hat{n}} + jk\;\tilde{p}'_s\,G\left(\frac{\partial\hat{r}}{\partial\hat{n}} + 2\,\mathbf{M}\cdot\mathbf{n}\right)\right]e^{-jk\hat{r}}\,\mathrm{d}\mathcal{S}(\mathbf{y}) \tag{C.4}$$

with boundary condition of Neumann type. If the body is at rest, the Neumann boundary condition reads $\partial p'_s/\partial n = -\partial p'_i/\partial n$, whereas for a moving body the following condition derived by linearization

of the Euler equation about the steady flow holds

$$\frac{\partial p'_s}{\partial n} = -\frac{\partial p'_i}{\partial n} - \rho_0 \{[(\Delta \mathbf{v} \cdot \nabla_t)\,\mathbf{n}] \cdot \mathbf{v}_p + [(\mathbf{v}_p \cdot \nabla_t)\,\mathbf{n}] \cdot \Delta \mathbf{v}\} + \left(\frac{p'_i}{{c_0}^2} + \frac{p'_s}{{c_0}^2} \right) [(\Delta \mathbf{v} \cdot \nabla_t)\,\mathbf{n}] \cdot \Delta \mathbf{v} \quad \text{(C.5)}$$

where ∇_t denotes tangential gradient operator, $\Delta \mathbf{v} = \mathbf{v}_{_B} - \mathbf{v}_{st}$ and $\mathbf{v}_p = \nabla(\phi_i + \phi_s)$ is provided by the VP solution (or approximated as $\mathbf{v}_p \approx \nabla \phi_i$). Alternatively, the boundary condition for moving body might be obtained through one of the approaches available in the literature for the evaluation of the gradient of the acoustic pressure [31, 32].

For the numerical solution of the integral formulation in Eq. (C.4), a zero-th order boundary element method similar to that described in Section II.B is applied.

FWHE formulation. The boundary integral formulation for sound scattering based on the solution of the Ffowcs-Williams and Hawkings equation has been developed in Ref. [11], through application of the boundary integral methodology presented in Refs. [14, 27]. Considering a rigid body in uniform translation impinged by an arbitrary incident acoustic disturbance, assuming an impermeable body surface, neglecting the source field terms in Eq. (C.3), and observing that for small perturbations, $\hat{p} \approx p'$, it provides the following frequency-domain, fully-linear FWHE scattering boundary integral representation in the BFR

$$\tilde{p}'_s(\mathbf{x}, k) = -\int_{\mathcal{S}} \left[\tilde{p}'_i \frac{\partial G}{\partial n} - jk\, \tilde{p}'_i\, G\, \frac{\partial \hat{r}}{\partial n} \right] e^{-jk\hat{r}} \mathrm{d}\mathcal{S}(\mathbf{y}) - \int_{\mathcal{S}} \left[\tilde{p}'_s \frac{\partial G}{\partial n} - jk\, \tilde{p}'_s\, G\, \frac{\partial \hat{r}}{\partial n} \right] e^{-jk\hat{r}} \mathrm{d}\mathcal{S}(\mathbf{y}) \quad \text{(C.6)}$$

with forcing terms related to the incident field.

For the numerical solution of the integral formulation in Eq. (C.6), a zero-th order boundary element method similar to that described in Section II.B is applied.

Remark #1. Similarly to the VP approach, both LE and FWHE formulations, firstly, are applied as boundary integral equations to determine the solution over the scatterer surface through a boundary element method close to that described in Section II.B and, then, are used as boundary integral representations to calculate it everywhere in the exterior field.

Remark #2. Observing that the LE and FWHE fully-linear frequency-domain formulations neglect, respectively, the $H\nabla \cdot (\nabla \cdot \mathbf{T})$ and $\nabla \cdot [\nabla \cdot (H\,\mathbf{T})]$ field sources, their difference is represented by the fluctuating first-order perturbations from the surface terms in Eq. (C.2). These may become relevant in proximity of a moving scatterer surface, where the reference steady flow perturbation

may be not negligible.

Remark #3. Regarding the comparisons between the results provided by the pressure-based LE and FWHE formulations and those given by the VP approach, note that, for homentropic flows subject to small perturbations, p_i and p_s can be considered coincident with, respectively, p'_i and p'_s.

Remark #4. Considering that in a MFR the Bernoulli theorem for homentropic, potential flows subject to small perturbations yields

$$\hat{p} = -\rho_0 \left(\frac{\partial \phi}{\partial t} + \frac{v^2}{2} \right) \tag{C.7}$$

it is possible to prove that the field contributions neglected in the VP and LE fully-linear scattering formulations differ for fluctuating first-order perturbation contributions coming from the wave operator applied to the $v^2/2$ term. Indeed, reminding that $\hat{p} \approx p'$, using Eq. (1) written in the MFR, and combining with Eq. (C.1), the wave operator applied to Eq. (C.7) gives

$$\Box^2 p' = -\rho_0 \left[\frac{\partial}{\partial t} \left(\Box^2 \phi \right) + \Box^2 \left(\frac{v^2}{2} \right) \right] = \rho_0 \left[\frac{\partial \sigma}{\partial t} + \Box^2 \left(\frac{v^2}{2} \right) \right] = \nabla \cdot (\nabla \cdot \mathbf{T}) \,, \qquad \boldsymbol{\xi} \in \mathbb{R}^3 \backslash \mathcal{B} \tag{C.8}$$

Remark #5. The VP, LE and FWHE integral formulations for sound scattering presented in Eqs. (5), (C.4) and (C.6) are identically valid also for rigid scatterers subject to uniform rotation or uniform rotation combined with uniform axial translation (helicoidal motion): indeed, in these cases, although the Mach number vector, $\mathbf{M}$, varies from point to point in space, it remains constant in time as observed from the BFR, and this guarantees the applicability of the frequency-domain, integral equation approaches developed here. However, because of the rotational motion, different Green's function observer-source distance parameter, r_β, and time delay, θ, arise (the latter, not given in closed form) [27, 28].

ACKNOWLEDGMENTS

The work presented in this paper is part of the activities of Roma Tre University/CNR-INSEAN team within the project GARTEUR HC AG-24.

REFERENCES

[1] Crighton, D.G., and Leppington, F.G., "On the Scattering of Aerodynamic Noise," *Journal of Fluid Mechanics*, Vol. 46, No. 3, 1971, pp. 577-597. doi: 10.1017/S0022112071000715

[2] Schenck, H.A., "Improved Integral Formulation for Acoustic Radiation Problems," *Journal of the Acoustical Society of America*, Vol. 44, No. 1, 1968, pp. 41-58. doi: 10.1121/1.1911085

[3] Colton, D., and Kress, R., *Integral Equation Methods in Scattering Theory*, John Wiley & Sons, NY, 1983. doi: 10.1137/1.9781611973167

[4] Seybert, A.F., and Soenarko, B., "Radiation and Scattering of Acoustic Waves from Bodies of Arbitrary Shape in Three-Dimensional Half Space," *Journal of Vibration, Acoustics, Stress, and Reliability in Design*, Vol. 110, No. 1, 1988, pp. 112-117. doi: 10.1115/1.3269465

[5] Farassat, F., and Myers, M.K., "Extension of Kirchhoff's Formula to Radiation from Moving Surfaces," *Journal of Sound and Vibration*, Vol. 123, No. 3, 1988, pp. 451-460. doi: 10.1016/S0022-460X(88)80162-7

[6] Gaunaurd, G.C., "Elastic and Acoustic Resonance Wave Scattering," *Applied Mechanics Reviews*, Vol. 42, No. 6, 1989, pp. 143-192. doi: 10.1115/1.3152427

[7] Amini, S., and Harris, P.J., "A Comparison Between Various Boundary Integral Formulation of the Exterior Acoustic Problem," *Computational Methods in Applied Mechanics and Engineering*, Vol. 84, No. 1, 1990, pp. 59-75. doi: 10.1016/0045-7825(90)90089-5

[8] Amini, S., Harris, P.J., and Wilton, D.T., "Coupled Boundary and Finite Element Methods for the Solution of the Dynamic Fluid-Structure Interaction," *Lecture Notes in Engineering (Ed. C. A. Brebbia and S. A. Orszag*, Vol. 77, Springer Verlag, New York/Berlin, 1992. doi: 10.1007/978-3-642-51727-3

[9] Wang, T.Q., and Zhou, S., "Investigation on Sound Field Model of Propeller Aircraft Effect of Vibrating Fuselage Boundary," *Journal of Sound and Vibration*, Vol. 209, No. 2, 1998, pp. 299-316. doi: 10.1006/jsvi.1997.1232

[10] Kehr, Y.Z., and Kao, J.H., "Underwater Acoustic Field and Pressure Fluctuation on Ship Hull Due to Unsteady Propeller Sheet Cavitation," *Journal of Marine Science and Technology*, Vol. 16, No. 3, 2011, pp 241-253. doi:10.1007/s00773-011-0131-4

[11] Gennaretti, M., and Testa, C., "A Boundary Integral Formulation for Sound Scattered by Moving Bodies," *Journal of Sound and Vibration*, Vol. 314, Nos. 3-5, 2008, pp. 712-737. doi: 10.1016/j.jsv.2008.01.028

[12] Lee, S., Brentner, K.S., and Morris, P.J., "Acoustic Scattering in the Time Domain Using an Equivalent Source Method," *AIAA Journal*, Vol. 48, No. 12, 2010, pp. 2772-2780. doi: 10.2514/1.45132

[13] Mao, Y., Gu, Y., and Xu, C., "Validation of Frequency-Domain Method to Compute Noise Radiated from Rotating Source and Scattered by Surface," *AIAA Journal*, Vol. 54, No. 4, 2016, pp. 1188-1197. doi:10.2514/1.J053674

[14] Morino, L., and Gennaretti, M., "Toward an Integration of Aerodynamics and Aeroacoustics of Rotors," DGLR/AIAA Paper 92-02-003, DGLR/AIAA 14th Aeroacoustics Conference, Aachen, Germany, 1992.

[15] Taylor, K., "A Transformation of the Acoustic Equation with Implications for Wind-Tunnel and Low-Speed Flight Tests," *Proceedings of the Royal Society of London*, Vol. A363, 1978, pp. 271-281 doi: 10.1098/rspa.1978.0168

[16] Astley, R., and Bain, J., "A Three-Dimensional Boundary Element Scheme for Acoustic Radiation in Low Mach Number Flows," *Journal of Sound and Vibration*, Vol. 109, No. 3, 1986, pp. 445-465. doi:10.1016/S0022-460X(86)80381-9

[17] Tinetti, A.F., and Dunn, M.H., "Aeroacoustic Noise Prediction Using the Fast Scattering Code," AIAA Paper 2005-3061, 11th AIAA/CEAS Aeroacoustics Conference, Monterey, California, 2005. doi:10.2514/6.2005-3061

[18] Agarwal, A., and Dowling, A.P., "Low-Frequency Acoustic Shielding by the Silent Aircraft Airframe," *AIAA Journal*, Vol. 45, No. 2, 2007, pp. 358365. doi:10.2514/1.19351

[19] Mancini, S., Astley, R.J., Sinayoko, S., Gabard, G., and Tournour, M., "An integral formulation for wave propagation on weakly non-uniform potential flows," *Journal of Sound and Vibration*, Vol. 385, 2016, pp. 184-201. doi:10.1016/j.jsv.2016.08.025

[20] Karimi, M., Croaker, P., Peake, N., and Kessissoglou, N., "Acoustic Scattering for Rotational and Translational Symmetric Structures in Nonuniform Potential Flow," *AIAA Journal*, Vol. 55, No. 10, 2017, pp. 3318-3327. doi: 10.2514/1.J055844

[21] Iemma, U., and Gennaretti, M. "Reduced-Order Modeling for Linearized Aeroelasticity of Fixed Wings in Transonic Flight," *Journal of Fluid and Structures*, Vol. 21, No. 3, 2001, pp. 243-255. doi:10.1016/j.jfluidstructs.2005.05.014

[22] Myers, M.K., and Hausmann, J.S., "Computation of Acoustic Scattering from a Moving Rigid Surface," *Journal of the Acoustical Society of America*, Vol. 91, No. 5, 1992, pp. 2594-2605. doi:10.1121/1.402996

[23] Vaidya, P.G., "Propagation of Sound in Flows Containing Mean Flow Gradients," AIAA Paper 81-1987, 7th AIAA Aeroacoustics Conference, Palo Alto, California, 1981. doi:10.2514/6.1981-1987

[24] Colton, D., and Kress, R., *Integral Equation Methods in Scattering Theory*, John Wiley & Sons, New York, 1983.

[25] Schenck, H.A., "Improved Integral Formulation for Acoustic Radiation Problems," *Journal of the Acous-*

tical Society of America, Vol. 44, No. 1, 1968, pp. 41-58. doi:10.1121/1.1911085

[26] Gennaretti, M., and Iemma, U., "Aeroacoustoelasticity in State-Space Format Using CHIEF Regularization," *J. of Fluids and Structures*, Vol. 17, No. 7, 2003, pp. 983-999. doi:10.1016/S0889-9746(03)00046-X

[27] Morino, L., and Gennaretti, M., "Boundary Integral Equation Methods for Aerodynamics," in: S.N. Atluri (Ed.), Computational Nonlinear Mechanics in Aerospace Engineering, *Progress in Astronautics and Aeronautics*, Vol. 146, AIAA, 1992. doi: 10.2514/5.9781600866180.0279.0320

[28] Gennaretti, M., Luceri, L., and Morino, L., "A Unified Boundary Integral Methodology for Aerodynamics and Aeroacoustics of Rotors," *J. of Sound and Vibration*, Vol. 200, No. 4, 1997, pp. 467-489. doi: 10.1006/jsvi.1996.0713

[29] Lighthill, M.J., "On Sound Generated Aerodynamically I. General Theory," *Proceedings of the Royal Society A*, Vol. 211, No. 1107, 1952, pp. 564-587. doi: 10.1098/rspa.1952.0060

[30] Ffowcs Williams, J.E., and Hawkings, D.L., "Sound Generated by Turbulence and Surfaces in Arbitrary Motion," *Philosophical Transactions of the Royal Society A*, Vol. 264, No. 1151, 1969, pp. 321-342. doi: 10.1098/rsta.1969.0031

[31] Farassat, F., and Brentner, K.S., "The Derivation of the Gradient of the Acoustic Pressure on a Moving Surface for Application to the Fast Scattering Code (FSC)," *NASA TM-2005-213777*, 2005.

[32] Bi, C.-X., Wang, Z.-H., and Zhang X.-Z., "Analytic Time-Domain Formulation for Acoustic Pressure Gradient Prediction in a Moving Medium," *AIAA Journal*, Vol. 55, No. 8, 2017, pp. 2607-2616. doi: 10.2514/1.J055630